Available online at www.sciencedirect.com
ScienceDirect
Journal of Power Sources 175 (2008) 26–32
JOURNAL OF POWER SOURCES
www.elsevier.com/locate/jpowsour

Pd nanoparticles supported on functionalized multi-walled carbon nanotubes (MWCNTs) and electrooxidation for formic acid

Sudong Yang [a], Xiaogang Zhang [b,*], Hongyu Mi [a], Xiangguo Ye [a]

[a] *Institute of Applied Chemistry, Xinjiang University, Urumqi 830046, PR China*
[b] *College of Material Science and Engineering, Nanjing University of Aeronautics and Astronautics, Nanjing 210016, PR China*

Received 28 July 2007; received in revised form 26 September 2007; accepted 26 September 2007
Available online 2 October 2007

Abstract

To improve the utilization and activity of anodic catalysts for formic acid electrooxidation, palladium (Pd) particles were loaded on the MWCNTs, which were functionalized in a mixture of 96% sulfuric acid and 4-aminobenzenesulfonic acid, using sodium nitrite to produce intermediate diazonium salts from substituted anilines. The composition, particle size, and crystallinity of the Pd/f-MWCNTs catalysts were characterized by X-ray diffraction (XRD), high-resolution transmission electron microscopy (HRTEM) and energy dispersive spectroscopy (EDS) measurements. The electrocatalytic properties of the Pd/f-MWCNTs catalysts for formic acid oxidation were investigated by cyclic voltammetry (CV) and linear sweep voltammetry (LSV) in 0.5 mol L^{-1} H_2SO_4 solution. The results demonstrated that the catalytic activity was greatly enhanced due to the improved water-solubility and dispersion of the f-MWCNTs, which were facile to make the small particle size (3.8 nm) and uniform dispersion of Pd particles loading on the surface of the MWCNTs. In addition, the functionalized MWCNTs with benzenesulfonic group can provide benzenesulfonic anions in aqueous solution, which may combine with hydrogen cation and then promote the oxidation of formic acid reactive intermediates. So the Pd/f-MWCNTs composites showed excellent electrocatalytic activity for formic acid oxidation.

Keywords: DFAFC; Functionalized MWCNTs; Palladium nanoparticles; Electrocatalysis; Formic acid electrooxidation

1. Introduction

Recently, the advantages of a direct formic acid fuel cell (DFAFC) have being progressively recognized compared to a direct methanol fuel cell (DMFC) [1]. For example, formic acid is non-toxic and is not easily burned. The optimal operating concentration of formic acid can be as high as 20 mol L^{-1} [2], while the best concentration of methanol in a DMFC is only about 2 mol L^{-1}. Thus, the energy density of DFAFC can be higher than that of DMFC. In addition, the penetration efficiency of formic acid through the Nafion membrane is much lower than that of methanol due to the repulsion between $HCOO^-$ and SO_3^- ions in the Nafion membrane [3]. To increase the catalytic activity of formic acid electrooxidation, an enormous effort has been devoted towards the development of catalysts. These catalysts include palladium and palladium-based alloy catalysts [4,5]. In fact, the choice of a suitable catalyst support is an important factor that may affect the performance of electrocatalysts owing to interactions and surface reactivity [6,7].

The tubular structure of carbon nanotubes makes them unique among different forms of carbon, and they can thus be exploited as an alternative material for catalyst support in heterogeneous catalysis [8] and in fuel cells due to the high surface area, excellent electronic conductivity, and high chemical stability [9–18]. Wildgoose et al. reviewed the recent developments in this area by exploring the various techniques to functionalize the carbon nanotubes with metals and other nanoparticles and the diverse applications of the resulting materials [19]. However, the applications of CNTs have been impeded by their poor solubility in solvents and polymers, which originated from strong van der Waals attractions among CNTs. Without the surface modification, most of CNTs lack sufficient binding sites for anchoring precursor metal ions or metal nanoparticles, which usually lead to poor dispersion and aggregation of metal

* Corresponding author. Tel.: +86 2552112902; fax: +86 2552112626.
E-mail address: azhangxg@163.com (X. Zhang).

0378-7753/$ – see front matter © 2007 Elsevier B.V. All rights reserved.
doi:10.1016/j.jpowsour.2007.09.080

nanoparticles, especially at high loading conditions. Therefore, functionalization of CNTs is generally prerequisite to further applications.

The functionalization of CNTs can be categorized into covalent and non-covalent functionalization, according to the nature of the interaction between CNTs and functional groups. To introduce more binding sites and surface anchoring groups, an acid oxidation process was very frequently adopted to treat CNTs in a refluxed, mixed acid aqueous solution at high temperatures (90–140 °C), which introduces surface-bound polar hydroxyl and carboxylic acid groups for subsequent anchoring and reductive conversion of precursor metal ions to metal nanoparticles. Recently, Tour and co-workers [20,21] reported the functionalization of CNTs using sodium nitrite to produce intermediate diazonium salts from substituted anilines can form benzenesulfonic group on the surface of CNTs, which improve the solubility in water. To the best of our knowledge, up to now, there have been no reports of using benzenesulfonic functionalized CNTs as the support for Pd nanoparticles in DFAFC.

In this paper, we demonstrate well dispersed reduction of Pd nanoparticles on the surface of benzenesulfonic functionalized MWCNTs from $PdCl_2$ aqueous solution by using $NaBH_4$ at room temperature. This method of catalyst preparation was performed in absence of any surfactant or organic additive. The synthesized Pd/f-MWCNTs electrocatalysts were characterized by the XRD, HRTEM and EDS. The electrocatalytic activities of the catalysts were examined by cyclic voltammetry and linear sweep voltammetry in 0.5 mol L^{-1} H_2SO_4 solution.

2. Experimental section

2.1. Reagent

MWCNTs were purchased from Shenzhen Nanotech Port Co., Ltd., China. The diameter and length ranged between 20–40 nm and 1–2 μm, respectively. Nafion (5 wt% in alcohols) was purchased from Aldrich. All the other reagents used were analytic grade and without further purification. All solutions were prepared with deionized water of a resistivity not less than 18.32 MΩ cm from an Ampeon 1810-B system (Sichuan, China).

2.2. Purification of raw MWCNTs (p-MWCNTs)

The MWCNTs were purified by the ultrasonic treatment for 1 h, refluxed with concentrated nitric acid at 373 K for 12 h, then washed and filtered with deionized water. The filtrate cake was dried in air at 353 K for 12 h [22].

2.3. Functionalization of MWCNTs (f-MWCNTs)

The procedures of benzenesulfonic functionalized MWCNTs have been reported as described elsewhere [18]. The detailed process was as follows: a mixture of 96% H_2SO_4 (150 mL) with MWCNTs (200 mg, 16 mmol) and $(NH_4)_2S_2O_8$ (100 g, 0.44 mol) was mixed with magnetic stirring (6 h). Once the mixture was visibly dispersed (no large particulates were visible), the substituted 4-aminobenzenesulfonic acid (5.54 g, 0.032 mol) was added and homogenization was continued for 2 h in order to effectively disperse the aniline throughout the mixture. This was followed by addition of solid $NaNO_2$ (2.208 g, 0.032 mol) and slow addition of 2,2-azobisisobutyronitrile (1.2 g, 0.4 mmol). The mixture was then placed in an oil bath at 80 °C and homogenization was continued for 6 h. The resulting product was filtered and washed with deionized water, acetone, and fresh *N*,*N*-dimethylformamide (DMF) then dried at 50 °C for 24 h in a vacuum oven.

2.4. Preparation of catalysts

f-MWCNTs supported Pd catalysts were synthesized at room temperature by using $NaBH_4$ as a reductive agent. Scheme 1 presents the synthesis procedure of the Pd/f-MWCNTs. Equimolar quantities of $PdCl_2$ were dissolved in deionized water and then the f-MWCNTs was added into this solution. The $NaBH_4$ solution ($NaBH_4$/metal molar ratio = 10) was slowly dropped into this mixture and vigorously stirred for 12 h. The resulting slurry was filtered, washed thoroughly with deionized water and then dried in a vacuum oven. The metal loading on MWCNTs was determined to be 20 wt%. For comparation, the Pd/p-MWCNTs and Pd/raw-MWCNTs(Pd/r-MWCNTs) catalysts were obtained as the same procedure as that for the Pd/f-MWCNTs catalyst.

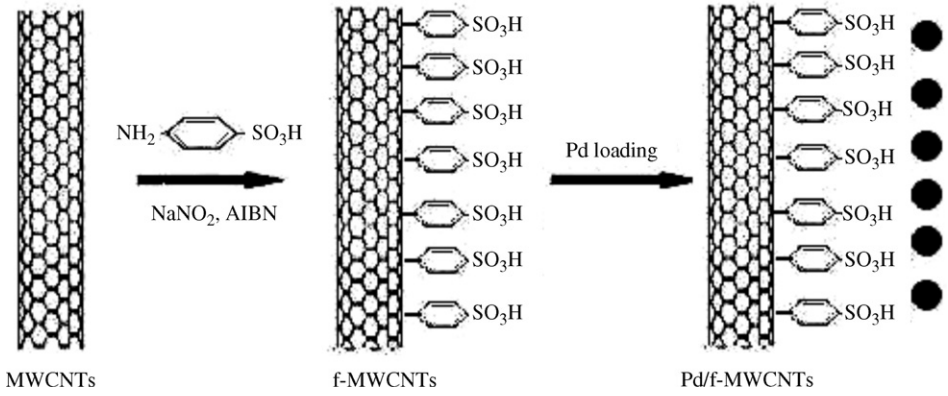

Scheme 1. Illustration of the synthesis procedure of the Pd/f-MWCNTs catalysts.

2.5. Preparation of electrode

Glassy carbon (GC) working electrodes, 5 mm in diameter (electrode area 0.2 cm^2), polished with 0.05 μm alumina to a mirror-finish before each experiment, were used as substrates for the MWCNTs supported catalysts. For the electrode preparation, typically, 5 mg electrocatalysts were added into 1 mL 0.05 wt% Nafion solution, and then the mixture was treated 1 h with ultrasonication for uniform dispersion. A measured volume (30 μL) of this mixture was dropped by a micropipette onto the top surface of the GC electrode. The as-obtained catalysts modified GC electrode was employed as the working electrode in our experiments.

2.6. Instrument and measurement

X-ray diffraction (XRD) analysis of the catalyst was carried out on Bruker D8-ADVANCE diffractometer with Cu Kα radiation of wavelength $\lambda = 0.15418$ nm. The morphology of the catalyst was investigated using a high-resolution transmission electron microscope (HRTEM) images were taken on a FEI Tecnai G^2 20S-TWIN microscope operated at 200 kV. Sample preparation for HRTEM examination was involved the ultrasonic dispersion of the sample in ethanol, then placing a drop of the suspension on a copper grid covered with perforated carbon film. Energy dispersive spectroscopy (EDS) spectrum analysis was carried out with a FEI Tecnai G^2 20S-TWIN microscope as an energy-dispersive X-ray analyzer. Infrared spectra were recorded with a model 360 Nicolet AVATAR FT-IR spectrophotometer.

The CV and LSV were performed with CHI 660 electrochemical workstation (Shanghai, China) in the potential range of −0.2 to 0.8 V with use of a three-electrode test cell. A conventional three-electrode system was used with a modified GC electrode as working electrode (5 mm in diameter), a Pt wire as counter electrode and saturated calomel electrode (SCE) as reference electrode, respectively. All electrolytes were deaerated by bubbling N_2 for 20 min and protected with a nitrogen atmosphere during the entire experimental procedure. All experiments were carried out at a temperature of 25 ± 1 °C.

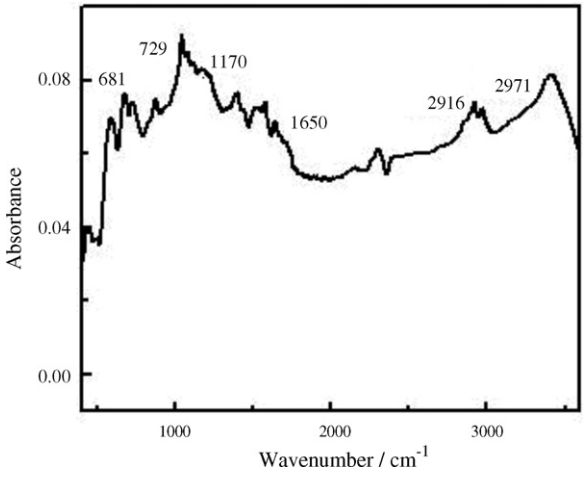

Fig. 1. IR spectrum of f-MWCNTs.

3. Results and discussion

3.1. Infrared (IR) analysis of f-MWCNTs

The possibility of functionalized MWCNTs with benzenesulfonic group has been examined by X-ray photoelectron spectroscopy (XPS) and high-resolution transmission electron microscopy analysis in other work [18,23]. Here we use IR analysis of f-MWCNTs to confirm such interaction. Fig. 1 is the IR spectrum of f-MWCNTs. The peaks at 729, 1650, 2916 and 2971 cm^{-1}, which are attributed to the adding of $–CH_2–$ group of the aromatic ring system. The peaks at 681 and 1170 cm^{-1} can be assigned to S–O group of sulfonate group. And from Fig. 1, we can see that there is no peak at 3200–3400 cm^{-1}, it indicates that there is no $–NH_2$ group on f-MWCNTs. So it confirms the reaction of functionalized MWCNTs according to Scheme 1. The f-MWCNTs were washed with acetone and DMF repeatedly in order to get rid of any impurity, thus it indicated that benzenesulfonic group were successfully modified on the surface of MWCNTs.

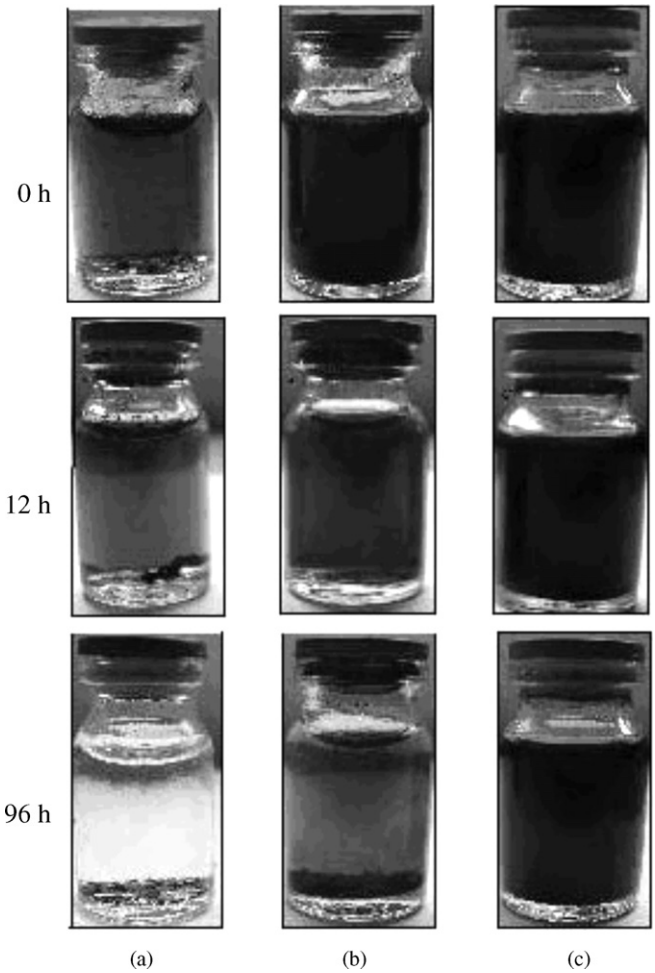

Fig. 2. Dispersibility of different MWCNTs in water: (a) r-MWCNTs; (b) p-MWCNTs; (c) Pd/f-MWCNTs.

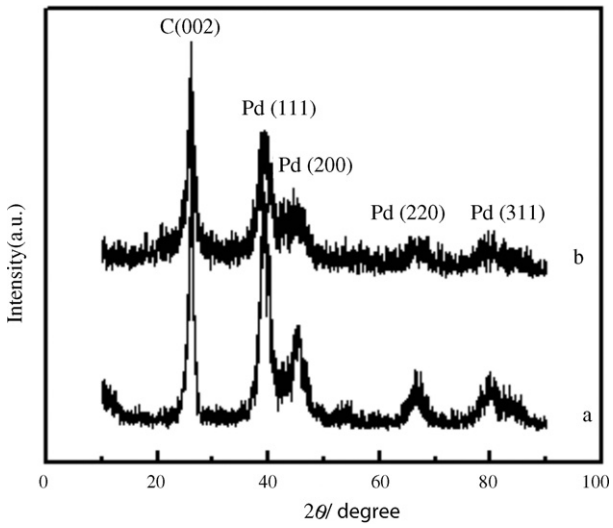

Fig. 3. XRD patterns of different catalysts: (a) Pd/p-MWCNTs; (b) Pd/f-MWCNTs.

3.2. Characterization of catalysts

The dispersibility of the r-MWCNTs, p-MWCNTs and f-MWCNTs in water were evaluated 96 h after the ultrasonic dispersion (Fig. 2). The r-MWCNTs and p-MWCNTs are not dispersed in water, as noticed by immediate precipitation of the aggregates of nanotubes are found at the bottom of vials (Fig. 2a and b), indicating the poor solubility of the r-MWCNTs and p-MWCNTs in water. By contrast, it is noted that the f-MWCNTs exhibit homogeneous dispersion in water even after 96 h (Fig. 2c), the solution become homogeneously ink-like, which confirms that the aggregates of nanotubes are not found at the bottom of vials. The result clearly indicated that the benzene-sulfonic functionalized MWCNTs were successfully formed, where hydrophilic benzene group improved the solubility of the MWCNTs.

XRD patterns reveal the bulk structure of the catalyst and its support. Fig. 3 shows the XRD patterns of the Pd/p-MWCNTs (curve a) and Pd/f-MWCNTs (curve b) catalysts. It can be seen that the first peak located at a 2θ value of about 26° is referred to graphite (0 0 2) plate of the MWCNTs support. The other four

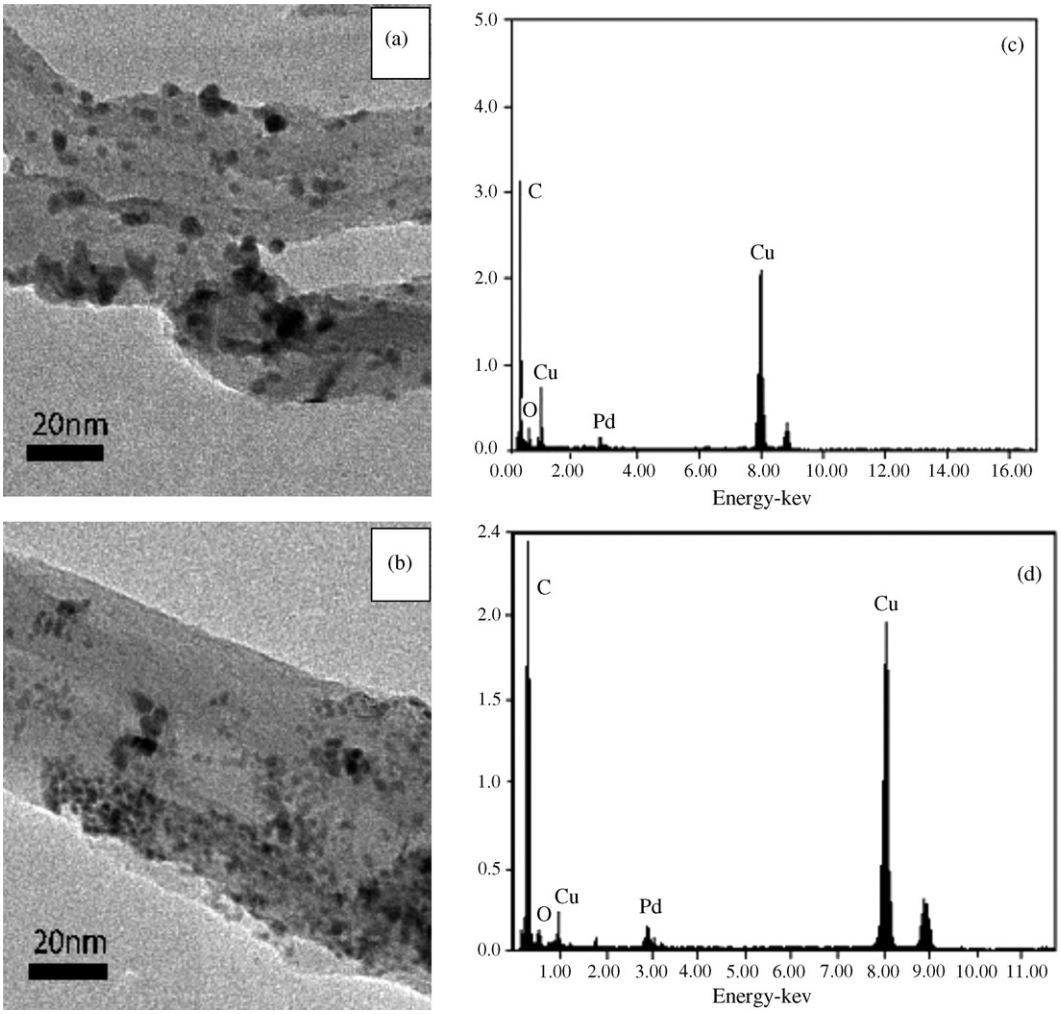

Fig. 4. HRTEM and EDS of different catalysts: Pd/p-MWCNTs (a and c), Pd/f-MWCNTs (b and d).

peaks are characteristic of face centered cubic (fcc) crystalline Pd (JCPDS, Card No. 05-0681), corresponding to the planes (1 1 1), (2 0 0), (2 2 0) and (3 1 1) at 2θ values of about 40°, 47°, 68° and 82°. The average size of the Pd particles on p-MWCNTs and f-MWCNTs is 4.2 and 3.8 nm, respectively, calculated from (2 2 0) peak by the Scherrer formula [24]. The results indicated that the Pd particles on f-MWCNTs in the Pd/f-MWCNTs catalysts were small than Pd/p-MWCNTs catalysts.

Fig. 4 shows the HRTEM and EDS images of the Pd/p-MWCNTs (a and c), Pd/f-MWCNTs (b and d) catalysts. The distribution of Pd nanoparticles on p-MWCNTs is not too much and large Pd clusters can be found in Fig. 4(a). However, a better dispersion of Pd nanoparticles on f-MWCNTs is shown in Fig. 4(c). Although agglomeration of Pd nanoparticles still exists, it can be seen from this image that too much very small black color Pd particles with more or less uniform dispersion formed on the outer walls of the MWCNTs. So the distribution of Pd nanoparticles on f-MWCNTs is greatly improved. It is due to the chemically active and hydrophilic surface of MWCNTs after benzenesulfonic functionalization. It should be mentioned that the f-MWCNTs supported Pd particles were synthesized completely in an aqueous phase by using $NaBH_4$ as a reducing agent. The f-MWCNTs should be easy to form the homogeneous solution in water, which is facile to load nanoparticles on the MWCNTs substrate. Unlike the method adopted in the present work, underwent severe aggregations and accumulated like clumps on the surface of the CNTs. The particle size of both catalysts observed from HRTEM measurement further confirms the calculated result from XRD analysis.

The EDS analysis confirmed the presence of Pd in the MWCNTs samples. The Cu derived from the copper lacy substrate used to hold the sample. In addition, O probably derived from high density surface functional groups, such as hydroxyl, carboxyl, and carbonyl groups formed on the outer walls of the MWCNTs after the purification or functionalization.

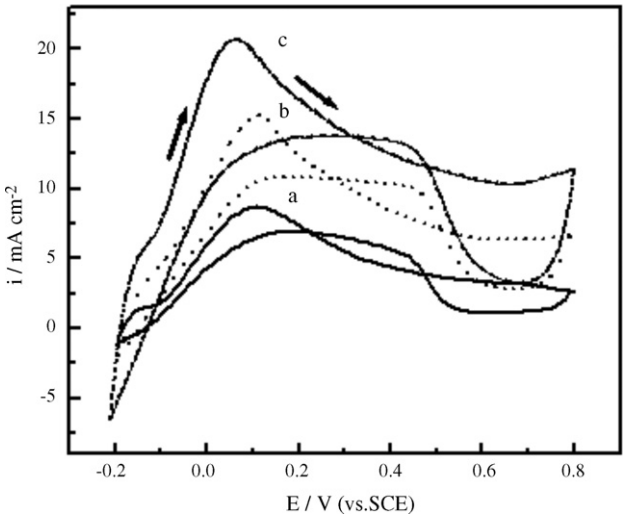

Fig. 6. Cyclic voltammograms of formic acid electrooxidation on different catalysts in 0.5 mol L^{-1} H_2SO_4 + 0.5 mol L^{-1} HCOOH at a scan rate of 50 mV s^{-1}. (a) Pd/r-MWCNTs; (b) Pd/p-MWCNTs; (c) Pd/f-MWCNTs.

3.3. Electrochemical properties of catalysts

The cyclic voltammograms of the Pd/p-MWCNTs (a) and Pd/f-MWCNTs (b) electrocatalysts are shown in Fig. 5. From Fig. 5, it can be seen that the area of hydrogen adsorption and desorption peak for Pd/f-MWCNTs electrocatalysts are bigger than that of the Pd/p-MWCNTs electrocatalysts. The large electrochemical specific surface may be due to the high dispersion and small size of Pd nanoparticles on the f-MWCNTs that functionalized with benzenesulfonic group.

The electrocatalytic activity of Pd/f-MWCNTs catalysts was evaluated by the electrochemical oxidation of formic acid with the prepared Pd/f-MWCNTs modified GC electrode as working electrode. For comparison, the Pd/p-MWCNTs and Pd/r-MWCNTs modified GC electrodes were also evaluated at the same condition. As shown in Fig. 6, the strong oxidation

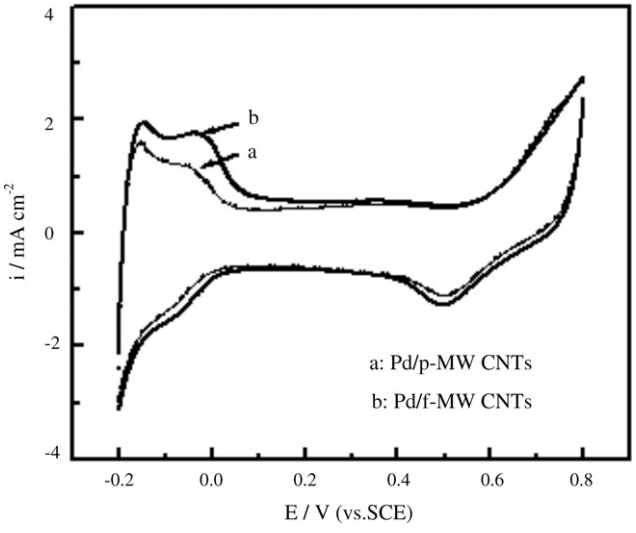

Fig. 5. Cyclic voltammograms of the different catalysts in 0.5 mol L^{-1} H_2SO_4 solution at a scan rate of 50 mV s^{-1}.

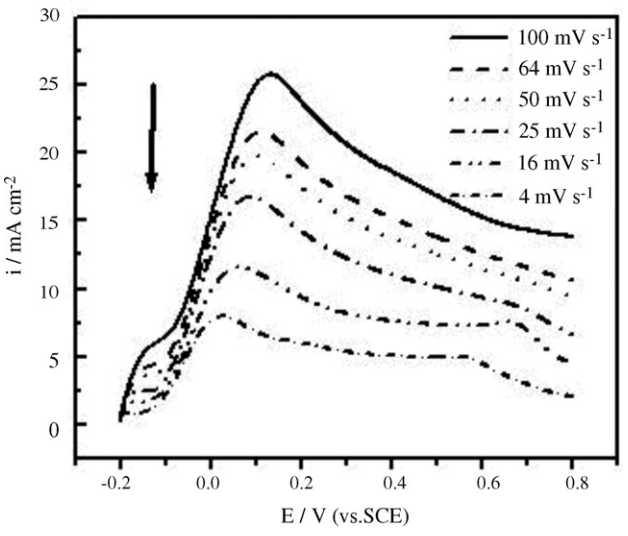

Fig. 7. The linear sweep voltammetry curves for formic acid oxidation on Pd/f-MWCNTs electrode at different scan rate.

Table 1
Electrochemical performances of formic acid oxidization on different catalysts

Different catalysts	E_p (V)	i_p (mA cm^{-2})
Pd/r-MWCNTs	0.11	8.66
Pd/p-MWCNTs	0.11	15.25
Pd/f-MWCNTs	0.06	20.68

peaks belong to the oxidation of formic acid and the corresponding intermediates [25]. The onset potential for formic acid oxidation on Pd/f-MWCNTs electrocatalyst showed a negative shift with a higher peak current density compared to that of Pd/p-MWCNTs and Pd/r-MWCNTs electrode as shown in Fig. 6. The positive scan oxidation peak current density and peak potential of the catalysts are shown in Table 1. On Pd/f-MWCNTs (c) catalysts, the peak potential of formic acid oxidation is more negative compared to Pd/r-MWCNTs (a) and Pd/p-MWCNTs (b). The anodic peak current density for Pd/f-MWCNTs (c) catalysts is 1.4 and 2.4 times of the Pd/MWCNTs (a) and Pd/p-MWCNTs (b), respectively. The improved performance of Pd/f-MWCNTs is due to the f-MWCNTs as the support, which has the high dispersivity, high loading capacity and excellent electrocatalytic performance in formic acid oxidation. Thus, the Pd/f-MWCNTs catalysts in present work can be expected to be effective electrode catalyst for the DFAFC.

Additionally, the anodic oxidation of formic acid is thought to occur via two parallel pathways. On Pd catalyst, formic acid would follow a different oxidation reaction pathway from that on Pt catalyst. Formic acid will adsorb rapidly on Pd catalyst and be oxidized to CO_2 directly without adsorbed CO as intermediate [26,27]

$$HCOOH \rightarrow HCOOH_{ads} \quad (1)$$

$$HCOOH_{ads} \rightarrow HCOO_{ads} + H^+ + e^- \quad (2)$$

$$HCOO_{ads} \rightarrow CO_2 + H^+ + e^- \quad (3)$$

This reaction pathway does not involve the participation of the water activation, so the onset oxidation potential for formic acid oxidation on Pd catalyst could be lowered. Toward to the Pd/f-MWCNTs catalysts, the functionalized MWCNTs with benzenesulfonic group, which can provide benzenesulfonic anions in solution, may contribute to the availability of the Pd active sites. On the other side, based on the reaction path (Eqs. (1)–(3)), the benzenesulfonic anions may combine with hydrogen cation that can promote the oxidation of formic acid reactive intermediate. So the Pd/f-MWCNTs catalysts have the excellent electrocatalytic performance in formic acid oxidation.

3.4. Kinetic characterization of formic acid electrooxidation on Pd/f-MWCNTs electrode

In order to investigate the kinetic characterization of formic acid oxidation on Pd/f-MWCNTs electrode, the effect of scan rate and formic acid concentration (C_{HCOOH}) on the behavior of formic acid oxidation were investigated. Figs. 7 and 8 show the effect of the scan rate on the electrooxidation of formic acid on Pd/f-MWCNTs electrode. From Fig. 7, the peak potential (the forward scan) increases with the increase of scan rate. It is indicated that the oxidation of formic acid is an irreversible electrode process. Additionally, in the range of 4–100 mV s^{-1}, the anodic peak current density is linearly proportional to the square root of scan rates (shown in Fig. 8), which suggests that the electrocatalytic oxidation of formic acid on Pd/f-MWCNTs modified electrode is a diffusion-controlled process. In addition, the peak potential (E_p) (the forward scan) increases with the increase of ν and linear relationship can be obtained between E_p and log(ν), as shown in Fig. 9. It further indicates that the oxidation of formic acid is an irreversible electrode process.

The formic acid concentration is also an important factor in the practical application of DFAFC. The effect of formic acid concentration on the anodic peak current density (i_p) and peak potential (E_p) was shown in Fig. 10A and B. From Fig. 10A, it can be seen that the anodic peak current density increases with the increase of formic acid concentration. This further indicates that the electrooxidation of formic acid at Pd/f-MWCNTs electrode is controlled by diffusion process. In

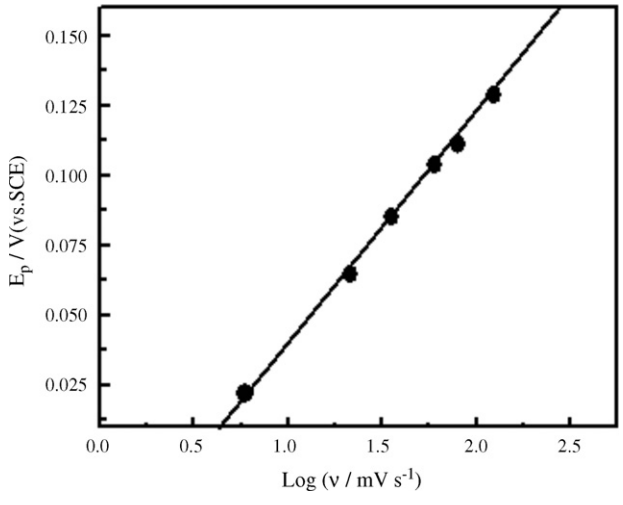

Fig. 9. The plot of E_p vs. log ν. $C_{HCOOH} = 0.5$ mol L^{-1}.

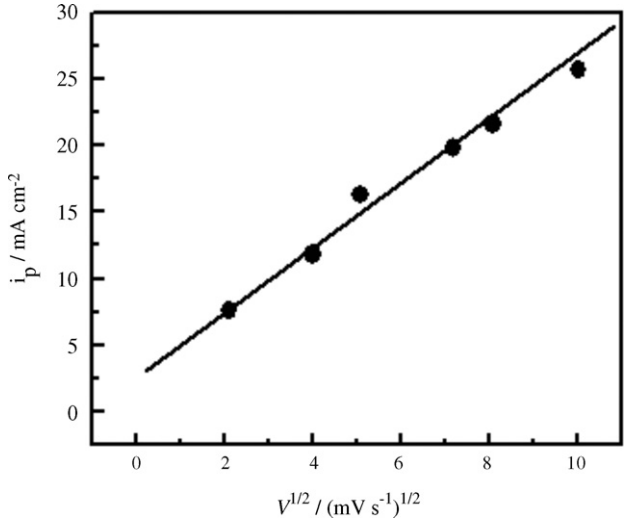

Fig. 8. Dependence of the peak current density on the square root of scan rates.

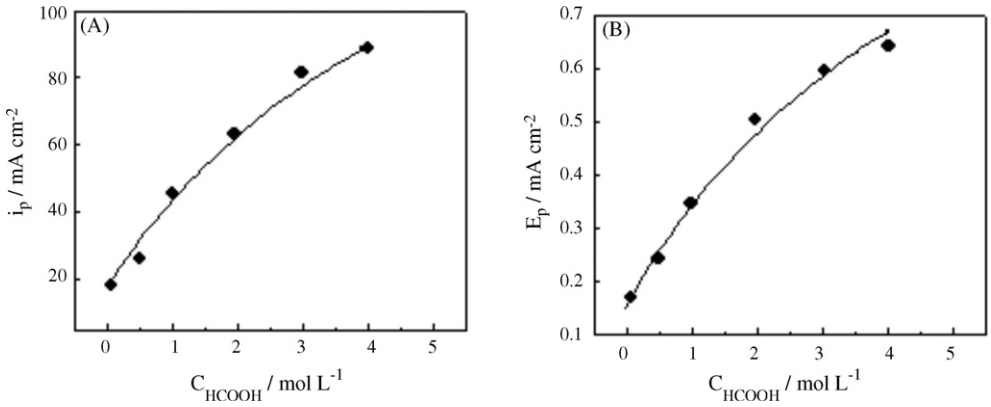

Fig. 10. Variation of the peak current density i_p (A) and the peak potential E_p (B) of HCOOH oxidation at the forward scan with C_{HCOOH}. The scan rate at 50 mV s^{-1}.

Fig. 10B, peak potential shifts towards positive direction when C_{HCOOH} increases. This may result from the following reasons: the increasing of the formic acid concentration will increase the poisoning rate of Pd catalyst and cause a more positive potential shift of the oxidative removal of the strongly adsorbed intermediates.

4. Conclusion

The higher dispersion of Pd nanoparticles supported on the f-MWCNTs were synthesized completely in an aqueous phase by a simple sodium borohydride reduction method at room temperature without using any stabilizer. The dispersion of f-MWCNTs and electrocatalytic properties of palladium nanoparticles on f-MWCNTs have been investigated. The Pd/f-MWCNTs composites showed excellent electrocatalytic activity for formic acid oxidation and good stability. This may be attributed to improved solubility of the f-MWCNTs, which was facile to make the small particle size and uniform dispersion of Pd particles loading on the outer walls of the MWCNTs. On the other side, the functionalized MWCNTs can provide benzenesulfonic anions in solution, which may combine with hydrogen cation that can promote the oxidation of formic acid reactive intermediate. This also implies that f-MWCNTs may be good candidates for catalyst supports because improving of the precious metal catalyst (Pd) dispersion in formic acid oxidation is an important practical consideration in fuel cell technology.

Acknowledgements

The authors gratefully acknowledge the support by National Basic Research Program of China (973 Program) (No. 2007CB209703), National Natural Science Foundation of China (Nos. 20403014, 20633040) and Natural Science Foundation of Jiangsu Province (BK2006196).

References

[1] S. Ha, B. Adams, R.I. Masel, J. Power Sources 128 (2004) 119–124.
[2] Y.W. Rhee, S. Ha, C. Rice, R.I. Masel, J. Power Sources 117 (2003) 35–38.
[3] A.V. Tripković, K.Dj. Popović, R.M. Stevanović, R. Socha, A. Kowal, Electrochem. Commun. 8 (2006) 1492–1498.
[4] L.L. Zhang, T.H. Lu, J.C. Bao, Y.W. Tang, C. Li, Electrochem. Commun. 8 (2006) 1625–1627.
[5] X.G. Li, I.M. Hsing, Electrochim. Acta 51 (2006) 3477–3483.
[6] Y.Y. Mu, H.P. Liang, J.S. Hu, L. Jiang, L.J. Wan, J. Phys. Chem. B 109 (2005) 22212–22216.
[7] G. Wu, Y.S. Chen, B.Q. Xu, Electrochem. Commun. 7 (2005) 1237–1243.
[8] D.J. Guo, H.L. Li, J. Power Sources 160 (2006) 44–49.
[9] G. Che, B.B. Lakshmi, E.R. Fisher, C.R. Martin, Nature 393 (1998) 346–349.
[10] G. Che, B.B. Lakshmi, C.R. Martin, E.R. Fisher, Langmuir 15 (1999) 750–758.
[11] B. Rajesh, V. Karthik, S. Karthikeyan, K.R. Thampi, J.M. Bonard, B. Viswanathan, Fuel 81 (2002) 2177–2190.
[12] Z.L. Liu, X.H. Lin, J.Y. Lee, W.D. Zhang, M. Han, L.M. Gan, Langmuir 18 (2002) 4054–4060.
[13] W.Z. Li, C.H. Liang, W.J. Zhou, J.S. Qiu, Z.H. Zhou, G.Q. Sun, J. Phys. Chem. B 107 (2003) 6292–6299.
[14] T. Matsumoto, T. Komatsu, H. Nakano, K. Arai, Y. Nagashima, E. Yoo, T. Yamazaki, M. Kijima, H. Shimizu, Y. Takasawa, J. Nakamura, Catal. Today 90 (2004) 277–281.
[15] C. Kim, Y.J. Kim, Y.A. Kim, T. Yanagisawa, K.C. Park, M. Endo, M.S. Dresselhaus, J. Appl. Phys. 96 (2004) 5903–5905.
[16] Y.C. Xing, J. Phys. Chem. B 108 (2004) 19255–19259.
[17] C. Wang, M. Waje, X. Wang, J.M. Tang, C.R. Haddon, Y. Yan, Nano Lett. 4 (2004) 345–348.
[18] M. Carmo, V.A. Paganin, J.M. Rosolen, E.R. Gonzalez, J. Power Sources 142 (2005) 169–179.
[19] G.G. Wildgoose, C.E. Banks, R.G. Compton, Small 2 (2006) 182–193.
[20] J.L. Hudson, M.J. Casavant, J.M. Tour, J. Am. Chem. Soc. 126 (2004) 11158–11159.
[21] J.J. Stephenson, J.L. Hudson, S. Azad, J.M. Tour, Chem. Mater. 18 (2006) 374–377.
[22] J.S. Huang, X.G. Zhang, Acta Phys. Chim. Sin. 22 (2006) 1551–1554.
[23] F. Barroso-Bujans, J.L.G. Fierro, S. Rojas, S. Sánchez-Cortes, M. Arroyo, M.A. López-Manchado, Carbon 45 (2007) 1669–1678.
[24] V. Radmilovic, H.A. Gasteiger, P.N. Ross, J. Catal. 154 (1995) 98–106.
[25] J.W. Guo, T.S. Zhao, J. Prabhuram, C.W. Wong, Electrochim. Acta 50 (2005) 1973–1983.
[26] J.D. Lović, A.V. Tripković, S.Lj. Gojković, K.Dj. Popović, D.V. Tripković, P. Olszewski, A. Kowal, J. Electroanal. Chem. 581 (2005) 294–302.
[27] H.Q. Li, G.Q. Sun, Q. Jian, M.Y. Zhu, S.G. Sun, Q. Xin, Electrochem. Commun. 9 (2007) 1410–1415.